P-ISSN 2586-9000
E-ISSN 2586-9027
Homepage : https://tci-thaijo.org/index.php/SciTechAsia
Science & Technology Asia
Vol.25 No.1 January - March 2020
Page: [11-18]
Original research article

Influences of Polarization on Two Equal Semi-permeable Cracks in a Piezoelectric Media

Kamlesh Jangid[1], Devendra Kumar[2], Jagdev Singh[3,*]

[1] *Department of Mathematics, Rajasthan Technical University, Kota-324010, India*
[2] *Department of Mathematics, University of Rajasthan, Jaipur-302004, India*
[3] *Department of Mathematics, Faculty of Science, JECRC University, Jaipur-303905, India*

Received 18 September 2019; Received in revised form 8 January 2020
Accepted 11 January 2020; Available online 26 March 2020

ABSTRACT

In this paper, the influence of arbitrary poling direction on a cracked piezoelectric medium is studied. For this purpose, an infinite piezoelectric plate cut along to equal semi-permeable collinear cracks is considered. Stroh's formalism and complex variable technique are used to formulate the problem. The closed-form analytical expressions are derived for the various fracture parameters viz. crack opening displacement, crack opening potential drop, intensity factors, and energy release rate. Moreover, the quadratic equation is derived to find the electric displacement inside the crack gap media. For a poled *PZT-5H* ceramic plate, an illustrative numerical investigation is implemented to demonstrate the effect of arbitrary polarization on the various fracture parameters.

Keywords: Multiple cracks; Piezoelectric ceramics; Polarization; Semi-permeable; Stroh's formalism

1. Introduction

Piezoelectric materials have been widely used in electromechanical gadgets, such as sensors, actuators or transducers, due to the coupling effect between mechanical and electrical characteristics. More and more consideration has been given to investigating deformities in piezoelectric media and structures. However, the presence of cracks is seen to reduce the strength of the ceramics considerably. And the effect of mechanical and electrical loading on crack opening is noticeable.

Many researchers [1–9] have explored a wide variety of crack problems for piezoelectric ceramics with impermeable, permeable electrical conditions on the crack face. These conditions give a higher and

***Corresponding author:** jagdevsinghrathore@gmail.com **doi:** 10.14456/scitechasia.2020.2

lower estimate of the rate of release of energy. In any case, semi-permeable crack face boundary condition is observed to give progressively precise results. These can be characterized within the crack gap with non-zero permittivity air/dielectric media as

$$D_2^+ = D_2^- = D = -\gamma_c \frac{\Delta\phi(x_1)}{\Delta u(x_1)}, \qquad (1.1)$$

where superscripts $^+$ and $^-$ represent, respectively, values on the upper and lower crack surfaces. Consider a crack along the x_1-axis; $\gamma_c = \gamma_r\gamma_0$ ($\gamma_0 = 8.85\times10^{-12}\ F/m$) is the electric permittivity of the medium between the crack faces; $\Delta\phi$ and Δu are the jumps of electric potential and crack opening displacement across the crack, respectively.

Many researchers [10–15] in their analysis used the semi-permeable boundary conditions. For the most part, for a single crack as it were, detailed semi-permeable crack problems have been researched. Hence, we considered in this paper two equal collinear crack cuts in an infinite piezoelectric plate with semi-permeable crack facing the prevailing electrical boundary conditions on crack faces.

It is also remarkable that in the material microstructure below Curie temperature a wide range of poled piezoelectric ceramics retain their aligned electrical dipole field. This direction of electrical poling affects the properties of the material and the behavior of fractures.

This paper addresses the question of arbitrary poling direction on a cracked piezoelectric media under semi-permeable crack boundary condition.

2. Fundamental formulation and solution methodology

The fundamental equations for linear piezoelectric media are defined as below:

- constitutive equations

$$\begin{aligned} \sigma_{ij} &= C_{ijks}\epsilon_{ks} - e_{sij}E_s, \\ D_i &= e_{kis}\epsilon_{ks} + \kappa_{is}E_s; \end{aligned} \qquad (2.1)$$

- kinematic equations

$$\begin{aligned} \epsilon_{ij} &= \frac{1}{2}(u_{i,j} + u_{j,i}), \\ E_i &= \phi_{,i}; \end{aligned} \qquad (2.2)$$

- equilibrium equations for stresses and electric displacements in the absence of body forces and free electric charges, may, respectively, be written as

$$\sigma_{ij} = 0,\ D_i = 0, \qquad (2.3)$$

where σ_{ij}, ϵ_{ij}, D_i and E_i denote the components of the stress, strain, electric displacement and electric field, respectively; C_{ijks} and e_{iks} denote the elastic and piezoelectric constants; and κ_{is} denotes the dielectric permittivities. Comma denotes partial differentiation with respect to argument following it; ϕ is the electric potential; where $i, j, k, s = 1, 2, 3$.

The constitutive equations above can be written as compact

$$\Xi_{i,j} = C_{ijkl}u_{k,j}, \qquad (2.4)$$

where

$$\Xi_{i,j} = \begin{cases} \sigma_{ij}, & i, j, k = 3 \\ D_j, & i = 4 \end{cases}$$

and material constant matrix $[C_{ijkl}]$ is defined in [16].

For the case of a 'θ' angle oriented poling direction with x_1-axis, the constitutive equations can be expressed as

$$\Xi_{i,j} = c_{ijkl}u_{k,j}, \qquad (2.5)$$

where

$$c_{ijkl} = \mathbf{m}C_{ijkl}\mathbf{m}^T,\ \mathbf{m} = \begin{pmatrix} \mathbf{m}_1 & \mathbf{0} \\ \mathbf{0} & \mathbf{m}_2 \end{pmatrix},$$

$\mathbf{m}_1$, $\mathbf{m}_2$ are taken from [16].

In accordance with Stroh's formalism, the general solution satisfying Eqs. ((2.1), (2.2) and (2.5)) can be written as

$$\mathbf{u}_{,1} = \mathbf{MG}(z) + \overline{\mathbf{MG}(z)}, \quad (2.6)$$
$$\mathbf{\Phi}_{,1} = \mathbf{NG}(z) + \overline{\mathbf{NG}(z)}, \quad (2.7)$$

where

$$\begin{aligned} \mathbf{M} &= (m_1, m_2, m_3, m_4), \\ \mathbf{N} &= (n_1, n_2, n_3, n_4), \\ \mathbf{G}(z) &= d\mathbf{g}(z)/dz, \\ \mathbf{g}(z_\alpha) &= [g_1(z_1), g_2(z_2), g_3(z_3), g_4(z_4)]^T, \\ z_\alpha &= x_1 + q_\alpha x_2, \end{aligned}$$

q_α is a non-real root of

$$|\mathbf{J} + q(\mathbf{K} + \mathbf{K}^T) + q^2\mathbf{L}| = 0 \quad (2.8)$$

and the matrices $\mathbf{J}$, $\mathbf{K}$ and $\mathbf{L}$ are given by

$$\mathbf{J} = c_{i1k1},\ \mathbf{K} = c_{i1k2},\ \mathbf{L} = c_{i2k2},$$

for all $i, k = 1, 2, 3$ and $\mathbf{\Phi}$ is the generalized stress function such that

$$\boldsymbol{\sigma}_2 = [\sigma_{2j}, D_2]^T = \mathbf{\Phi}_{,1},$$
$$\boldsymbol{\sigma}_1 = [\sigma_{1j}, D_1]^T = -\mathbf{\Phi}_{,2}.$$

3. Statement of the problem

Let us consider that the whole plane x_1ox_2 is occupied by an infinite transversely isotropic piezoelectric plate, and the poling direction makes an angle with x_1-axis. The plate is cut along two equal L_1 and L_2 straight collinear cracks that occupy $[d, c]$ and $[-c, -d]$ on x_1-axis at the corresponding intervals. It is presumed that the crack surfaces are traction-free and that the semi-permeable boundary condition is presumed to be kept inside cracks. The mechanical stressand σ_{22}^∞ and the electrical displacement load D_2^∞ are prescribed at the remote boundary of the plate. Fig. 1. shows the schematic representation of the problem.

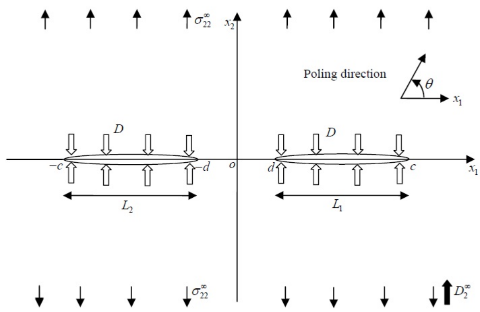

Fig. 1. Schematic representation of the problem.

Mathematically, the conditions of the physical boundary may be as follows:

(i) $\sigma_{2j}^+ = \sigma_{2j}^- = 0,\ D_2 = D$, on $L = L_1 \cup L_2$;

(ii) $\sigma_{22} = \sigma_{22}^\infty,\ D_2 = D_2^\infty$, for $|x_2| \to \infty$;

(iii) $u_j^+ = u_j^-,\ \sigma_{2j}^+ = \sigma_{2j}^-,\ D_2^+ = D_2^-,\ \phi^+ = \phi^-$, for $|x_1| < d,\ |x_1| > c$;

(iv) $\mathbf{\Phi}_{,1}^+ = \mathbf{\Phi}_{,1}^- = -\boldsymbol{V},\ \boldsymbol{V} = [0,\ \sigma_{22}^\infty,\ 0,\ D_2^\infty]^T$ for $d < |x_1| < c$,

where D is the electric flux through the crack regions, which can be determined with the help of the Eq. (1.1).

4. Solution of the problem

The continuity of generalized stress on the whole real x_1-axis implies that

$$[\boldsymbol{NG}(x_1) - \overline{\boldsymbol{NG}}(x_1)]^+ - [\boldsymbol{NG}(x_1) - \overline{\boldsymbol{NG}}(x_1)]^- = 0. \quad (4.1)$$

According to Muskhelishvili [17], its solution may be written as

$$\boldsymbol{NG}(z) - \overline{\boldsymbol{NG}}(z) =: I(z). \quad (4.2)$$

Using the principle of superposition, boundary conditions (i) and (iv) together with Eqs. (2.7) and (4.2) yield the following vector Hilbert problem

$$I^+(x_1) + I^-(x_1) = \boldsymbol{V}^0 - \boldsymbol{V},$$
$$\boldsymbol{V}^0 = [0, 0, 0, D]^T, \quad d < |x_1| < c. \quad (4.3)$$

Introducing a complex function vector

$$\boldsymbol{\Psi}(z) = [\Psi_1, \Psi_2, \Psi_3, \Psi_4]^T$$

as

$$\boldsymbol{\Psi}(z) = \boldsymbol{H}^R \boldsymbol{N} \boldsymbol{G}(z) \quad (4.4)$$

which together with Eq. (4.2) leads to the relation

$$I(z) = \Upsilon \boldsymbol{\Psi}(z), \quad (4.5)$$

where

$$\Upsilon = [\boldsymbol{H}^R]^{-1}, \ \boldsymbol{H}^R = 2\,\mathrm{Re}\,\boldsymbol{Y}, \ \boldsymbol{Y} = \mathrm{Im}(\boldsymbol{M}\boldsymbol{N}^{-1}).$$

Writing the second and fourth components of Eq. (4.3), the following two scalar Hilbert problems are obtained

$$\Upsilon_{22}[\Psi_2^+(x_1) + \Psi_2^-(x_1)] + \Upsilon_{24}[\Psi_4^+(x_1) + \Psi_4^-(x_1)] = -\sigma_{22}^{\infty}, \quad (4.6)$$

$$\Upsilon_{42}[\Psi_2^+(x_1) + \Psi_2^-(x_1)] + \Upsilon_{44}[\Psi_4^+(x_1) + \Psi_4^-(x_1)] = D - D_2^{\infty} \quad (4.7)$$

The solutions of the above Hilbert problems are written (using Muskhelishvili [17]) as

$$\Psi_2(z) = \frac{1}{2\Theta}\left(\Upsilon_{44}\sigma_{22}^{\infty} + (D - D_2^{\infty})\Upsilon_{24}\right)\left(\frac{z^2 - c^2\lambda^2}{X_1(z)} - 1\right), \quad (4.8)$$

$$\Psi_4(z) = \frac{1}{2\Theta}\left(\Upsilon_{42}\sigma_{22}^{\infty} + (D - D_2^{\infty})\Upsilon_{22}\right)\left(1 - \frac{z^2 - c^2\lambda^2}{X_1(z)}\right), \quad (4.9)$$

where

$$X_1(z) = \sqrt{(z^2 - d^2)(z^2 - c^2)},$$
$$\Theta = \Upsilon_{22}\Upsilon_{44} - \Upsilon_{24}\Upsilon_{42},$$
$$k^2 = 1 - (d/c)^2,$$
$$\lambda^2 = E(k)/F(k),$$

$F(k)$ and $E(k)$ are the complete elliptic integrals of first and second kinds, respectively.

5. Applications

The terms for crack opening displacement (COD), crack opening potential drop (COP), stress and electrical displacement intensity factors, mechanical and total release rates of energy are derived in this section.

We introduced the jump displacement vector, $\Delta\mathbf{u}_{,1}$ as

$$i\Delta\mathbf{u}_{,1} = i[u_{1,1}^+ - u_{1,1}^-, u_{2,1}^+ - u_{2,1}^-, u_{3,1}^+ - u_{3,1}^-, \phi^+ - \phi^-]^T, \quad (5.1)$$

where the symbol 'Δ' indicates the difference between the values on the upper and lower crack surfaces.

5.1 Crack opening displacement (COD)

The relative opening of the crack faces is obtained using the second component of Eq. (5.1), and substituting the value of $\Psi_2(z)$ from Eq. (4.8) and integrating, one obtains

$$\Delta u_2(x) = -\frac{c}{\Theta}\left(\Upsilon_{44}\sigma_{22}^{\infty} + (D - D_2^{\infty})\Upsilon_{24}\right)\left(\lambda^2 F(\tau, k) - E(\tau, k)\right), \quad (5.2)$$

where $\sin^2\tau = (c^2 - y^2)/(c^2 - d^2)$.

5.2 Crack opening potential drop (COP)

Comparing the fourth component of Eq. (5.1) and using the value of $\Psi_2(z)$ from Eq. (4.9) and integrating, one obtains the COP drop as

$$\Delta\phi(x) = -\frac{c}{\Theta}\left(\Upsilon_{42}\sigma_{22}^{\infty} + (D - D_2^{\infty})\Upsilon_{22}\right)\left(\lambda^2 F(\tau, k) - E(\tau, k)\right). \quad (5.3)$$

Remark 5.1. *The value of electric flux D is obtained by substituting the required values from Eq. (5.2) and Eq. (5.3) into Eq. (1.1) and solving the quadratic equation*

$$\eta_1 D^2 + \eta_2 D + \eta_3 = 0, \quad (5.4)$$

where $\eta_1 = \Upsilon_{24}$, $\eta_2 = \Upsilon_{44}\sigma_{22}^{\infty} - \Upsilon_{24}D_2^{\infty} - \Upsilon_{22}\gamma_c$, $\eta_3 = -\gamma_c(\Upsilon_{42}\sigma_{22}^{\infty} - \Upsilon_{22}D_2^{\infty})$. *For the required value of D, the root should be chosen for which COD is positive.*

5.3 Intensity factors (IFs)

Stress intensity factor, KI, and electric displacement intensity factor, KIV, at the crack tips x = d and x = c are given as

$$K_I(d) = -\sqrt{\frac{\pi}{d(c^2-d^2)}}\left(\sigma_{22}^{\infty} + (D - D_2^{\infty})\frac{\Upsilon_{24}}{\Upsilon_{44}}\right)(d^2 - c^2\lambda^2), \quad (5.5)$$

$$K_I(c) = \sqrt{\frac{\pi}{c(c^2-d^2)}}\left(\sigma_{22}^{\infty} + (D - D_2^{\infty})\frac{\Upsilon_{24}}{\Upsilon_{44}}\right)(c^2 - c^2\lambda^2), \quad (5.6)$$

$$K_{IV}(d), = \sqrt{\frac{\pi}{d(c^2-d^2)}}\left((D - D_2^{\infty}) + \sigma_{22}^{\infty}\frac{\Upsilon_{42}}{\Upsilon_{22}}\right)(d^2 - c^2\lambda^2), \quad (5.7)$$

$$K_{IV}(c) = -\sqrt{\frac{\pi}{c(c^2-d^2)}}\left((D - D_2^{\infty}) + \sigma_{22}^{\infty}\frac{\Upsilon_{42}}{\Upsilon_{22}}\right)(c^2 - c^2\lambda^2). \quad (5.8)$$

5.4 Energy release rate (ERR)

Mechanical energy release rate (MERR), G_M, and total energy release rate (TERR), G_T, at the inner and outer crack tips $x = d$ and $x = c$ calculated using formulae

$$G_M = \frac{1}{2}(H_{22}K_I^2 + H_{24}K_{IV}),$$
$$G_T = \frac{1}{2}(H_{22}K_I^2 + 2H_{24}K_{IV} + H_{44}K_{IV}^2). \quad (5.9)$$

6. Case study

An illustrative numerical case study is presented for PZT-5H ceramic plate to investigate the behaviour of poling direction on the fracture parameters viz. COD, COP, SIF, MEER and TERR. The material constants are given in Table 1. We assume the length of cracks, prescribed tension and electrical displacement load is 10mm, $\sigma_{22}^{\infty} = 1MPa$ and $D_2^{\infty} = 0.001$ C/m^2 respectively.

Table 1. Material parameters of PZT-5H

Material constants	PZT-5H
c_{11} $(10^{10}\ N/m^2)$	12.60
c_{12} $(10^{10}\ N/m^2)$	7.95
c_{13} $(10^{10}\ N/m^2)$	8.41
c_{33} $(10^{10}\ N/m^2)$	11.70
c_{44} $(10^{10}\ N/m^2)$	2.30
e_{13} (C/m^2)	-6.50
e_{33} (C/m^2)	23.30
e_{15} (C/m^2)	17.44
k_{11} $(10^{-10}\ C/(Vm))$	150.30
k_{33} $(10^{-10}\ C/(Vm))$	130

Fig. 2. shows the variation of COD for distinct poling angles over the crack surface. As the poling angle 'θ' increases from 0° to 90°, it is observed from the figure that COD increases. COD attains maximum value for 90° (if the direction of poling is perpendicular to the surface of the crack) and minimum value for 0° (if the direction of poling is parallel to the surface of the crack).

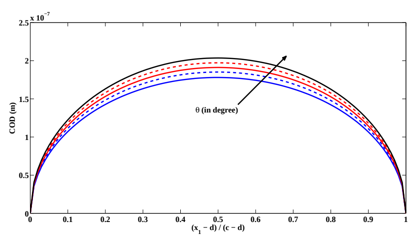

Fig. 2. COD versus θ

Fig. 3 shows the variation of COP drop over the crack surface for different poling angles. The figure shows that COP drop increases as the poling angle increases. COP drop attains maximum value for 90° and minimal value for 0°.

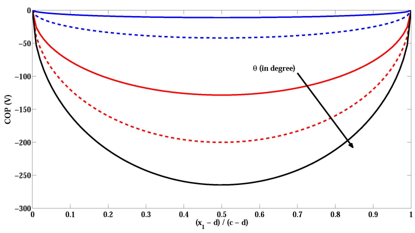

Fig. 3. COP versus θ

Fig. 4 and Fig. 5 depict the variation of K_{IV} and K_I for distinct poling angle at the internal and outer ends of the crack with regard to the electrical displacement load D_2^∞. It is observed that as D_2^∞ increases, K_{IV} and K_I also increase at both of the crack tips. Also K_{IV} and K_I are higher at the inner crack tip d as compared to that at outer crack tip c, as expected. It may also be noted from the figures that K_{IV} and K_I are maximum when poling direction is perpendicular to the crack face i.e., 90°. And it attains minimum value when poling direction is parallel to the crack face i.e., 0°.

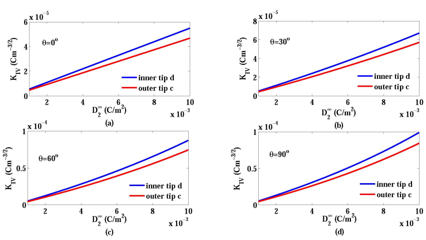

Fig. 4. K_{IV} versus D_2^∞ for different θ

Fig. 6 and Fig. 7, respectively, depict the behavior of MERR and TERR with respect to the variation in the non dimensional electric loading coefficient λ_d for different poling angles. It is observed that TERR and MERR are higher at the inner tip than those at the outer tip. It is noted from Fig. 6 that the MERR always increases by increasing electrical loadings λ_d, and decreases with respect to the decrease in electrical loadings. It may also be noted from Fig. 7(a) that the TERR decreases symmetrically for $\lambda_d = 0$. This shows that the TERR is independent of the direction of the applied electrical loading. This symmetrical point varies as poling angle changes.

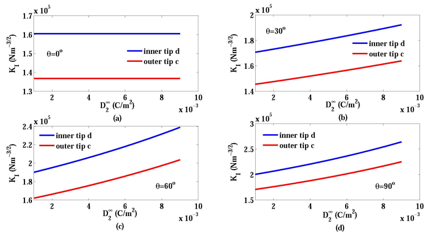

Fig. 5. K_I versus D_2^∞ for different θ

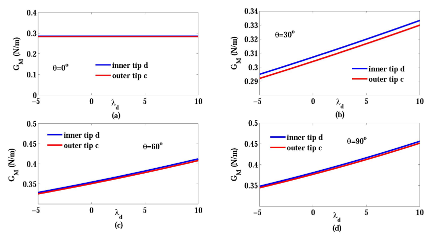

Fig. 6. G_M versus λ_d for different θ

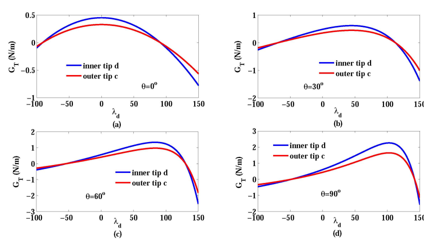

Fig. 7. G_T versus λ_d for different θ

7. Conclusion

The following conclusions are made from the analytical and numerical studies presented for the proposed two equal collinear semi-permeable cracks model with arbitrarily oriented electric poling in piezoelectric media:

- The various fracture parameters viz. COD, COP, IFs, MERR and TERR attained maximum values when the direction of poling was perpendicular to the crack faces. And these parameters attained minimum values when the direction of poling was moved along the length of the crack face.
- The IFs and MERR increase as the displacement of electric load increases and decrease as the displacement of electric load decreases.

References

[1] Sosa H. Plane problems in piezoelectric media with defects. Int J Solids Struct 1991;28:491-505.

[2] Zuo JZ, Sih GC. Energy density theory formulation and interpretation of cracking behavior for piezoelectric ceramics. Theo Appl Fract Mech 2000;34:17-33.

[3] Qi H, Fang DN, Yao Z. Analysis of electric boundary condition effects on crack propagation in piezoelectric ceramics. Acta Mech 2001;17:59-70.

[4] Beom HG, Atluri SN. Conducting cracks in dissimilar piezoelectric media. Int J Fract 2002;118:285-301.

[5] Beom HG. Permeable cracks between two dissimilar piezoelectric materials. Int J Solids Struct 2003;40: 6669-79.

[6] Zhou ZG, Wang B, Cao MS. The behavior of permeable multi-cracks in a piezoelectric material. Mech Res Commun 2003;30:395-402.

[7] Chen BJ, Liew KM, Xiao ZM. Unified electrical boundary conditions for a crack interacting with a dislocation in piezoelectric media. Int J Solids Struct 2005;42:5118-28.

[8] Chue CH, Weng SM. Fracture analysis of piezoelectric materials with an arbitrarily oriented crack using energy density theory. Comput Struct 2005;83:1251-61.

[9] Jelitto H, Kebler H, Schneider GA, Balke H. Fracture behavior of poled piezoelectric PZT under mechanical and electrical loads. J Euro Cera Soc 2005;25:749-57.

[10] Mcmeeking RM. Crack tip energy release rate for a piezoelectric compact tension specimen. Eng Fract Mech 1999;8:217-44.

[11] Landis CM. Energetically consistent boundary conditions for electromechanical fracture. Int J Solids and Struct 2004;37:4969-86.

[12] Ou ZC, Chen YH. On approach of crack tip energy release rate for a semipermeable crack when electromechanical loads become very large. Int J Fract 2003;133:89-105.

[13] Liu JY, Zhou ZG, Zhou BB. Basic solution of four 3-D rectangular limited-permeable cracks in piezoelectric materials. ZAMM J Appl Math Mech 2012;92:632-51.

[14] Bhargava RR, Jangid K, Verma PR. Two semi-permeable equal collinear cracks weakening a piezoelectric plate-A study using complex variable technique. ZAMM J Appl Math Mech 2013;95:66-76.

[15] Bhargava RR, Jangid K. Closed form solution for two unequal collinear semipermeable straight cracks in a piezoelectric media. Arch Appl Mech 2014;84:833-49.

[16] Jangid K, Bhargava RR. Influence of polarization on two unequal semi-permeable cracks in a piezoelectric media. Stren Frac Complex 2017;10:129-44.

[17] Muskhelishvili NI. Some Basic problems of Mathematical Theory of Elasticity. Noordhoff Leyden: Springer Netherlands; 1975.